Numerical Simulation and Bench Test of Crawler-Type Cotton Time-Delay Hole-Forming Device Based on RecurDyn-EDEM Coupling

Feng Pan , Jincheng Chen , Hualin Zhang , Baiwei Wang , Xizhen Jiang , Chao Ji *

Posted Date: 3 June 2024

doi: 10.20944/preprints202406.0097.v1

Keywords: cotton; crawler-type; delayed hole-forming device; coupling simulation; field experiment; soil bin test

Article

Numerical Simulation and Bench Test of Crawler-Type Cotton Time-Delay Hole-Forming Device Based on RecurDyn-EDEM Coupling

Feng Pan [1,3], Jincheng Chen [1,3], Hualin Zhang [1,2,3], Baiwei Wang [1,3], Xizhen Jiang [1,2,3] and Chao Ji [1,3]*

[1] Institute of Mechanical Equipment, Xinjiang Academy of Agricultural and Reclamation Science, Shihezi 832000, China; 17609922366@163.com (F.P.); shznkycjc@163.com (J.C.); 17867591817@163.com (H.Z.); 13359500372@163.com (B.W.); 19990891915@163.com (X.J.)

[2] College of Mechanical and Electrical Engineering, Shihezi University, Shihezi 832003, China

[3] Key Laboratory of Northwest Agricultural Equipment, Ministry of Agriculture and Rural Affairs, Shihezi 832003, China

* Correspondence: jicobear@163.com

Abstract: Addressing the significant challenge in high-speed cotton dibbling operations in Xinjiang—specifically, the duck bill's ("Duck bill" is a type of duck-billed bunch planting mechanism or component). shortened opening duration leading to seed throwing and floating—a new crawler-type delayed hole-forming mechanism has been designed. This mechanism extends the duck bill horizontally, thereby prolonging its opening time, enabling cotton sowing speeds of up to 6 km/h. Following agronomic principles for cotton planting, the overall layout of the crawler-type hole-forming mechanism, the structural parameters of the key components and the trajectory of the hole-forming are determined. We use the Discrete Element Method (DEM) and multi-body dynamics coupling method to simulate and analyze the motion process of the device. The fixed the tilt angle of the duck bill $\alpha(A)$, the depth of the duck bill hole-forming into the soil $h(B)$, and the angle of rotation of the moving duck bill $\beta(C)$ were taken as the experimental factors, with the longitudinal length of cotton seed hole (Y_1) and the hole-forming depth of cotton seed hole (Y_2) as the response values. The parameter range of each factor and the preliminary influence on the response value were determined through pre-experiments and single-factor simulation test. Based on RecurDyn-EDEM coupling, a quadratic regression orthogonal rotation combination simulation test was carried out. The results show that the order of the primary and secondary factors affecting the Y_1 of the time-lapse hole-forming device was: $A > C > B$. The order of primary and secondary factors affecting the Y_2 of the delayed hole forming device was: $B > C > A$. When the A was 2.4 °, the B was 42.4 mm, and the C was 30.5 °, the performance of the hole-forming was the best, and the Y_1 was 26.4 mm, and the Y_2 was 25.0 mm. The bench verification test results show that under the optimized combination of operating parameters, the average Y_1 was 29.1 mm, and the average Y_2 was 23.2 mm. Compared with the results of the previous coupled simulation model, the average relative errors of the two are 7.23 % and 4.36 %, respectively, indicating the accuracy and effectiveness of the established DEM simulation model and virtual test analysis. The hole-forming area and the opening time of the duck bill after the stable operation of the machine were recorded and measured. The calculated hole dislocation rate H_c was 4.33 %, which did not exceed the national standard requirement of 6 %. The qualified rate of hole distance H_x was 94.33 %, which was much higher than the national standard requirement of 80 %. The average opening time of the duck bill at a speed of 6 km/h is 0.45 s, which is much longer than the time required for cotton seeds to fall from the duck bill 0.11 s. It meets the requirements of high-speed cotton planting in China and facilitating advancements in future high-speed planter technology.

Keywords: cotton; crawler-type; delayed hole-forming device; coupling simulation; field experiment; soil bin test

 doi:10.20944/preprints202406.0097.v1

1. Introduction

Xinjiang is the main producing area of high-quality cotton in China. Improving the sowing speed and yield of cotton in Xinjiang has a significant strategic impact on ensuring the safety of China's cotton industry. Although Xinjiang is rich in light and heat resources, the farmland soil lacks moisture due to the climate. Plastic film mulching technology offers advantages such as rainwater harvesting and water storage,, increased temperature and soil moisture, improved soil physical and chemical properties and fertility, enhanced light conditions and weed growth inhibition [1,2]. To achieve stable yield and income, cotton planting in Xinjiangadopts film mulching planting method [3]. The sowing operation mainly relies on the film-laying precision seeder to complete the film hole sowing [4]. The hole planter is the core working part of the cotton planter, functioning as a seeding monomer that integrates the seed metering device, seed guiding tube, and hole-forming device.The hole-forming process is a key links of precision seeding on the film using the dibbler, and it is a prerequisite for the precise seeding of the dibbler. In Xinjiang, sowing operation is concentrated in mid to early April, with the sowing period typically lasting 7-10 days. Currently, the operating speed of the film-laying precision seeders widely used in Xinjiang is 3~4 km/h [5–7]. If the operation speed is increased, issues such as missed sowing, floating seed and dislocation can occur. To make the most of the agricultural season, more machinery and workers are needed, resulting in high operating costs. The primary the speed limitation of the current dibbler is that as the working speed of the planter increases,, the opening time of the duck bill hole-forming device is greatly reduced. This causes the moving duck bill parts in the hole-forming device to return prematurely, resulting in insufficient time for cotton seeds to fall, thus significant decreasing the quality of work.

The existing research and analysis of the hole-forming devices are mostly focused on transplanting machinery, with few studies on the duck bill hole-forming device. Xiang Wei et al. [8] developed a crawler rape transplanting hole-forming device. By analyzing the physical and mechanical properties of the soil, the friction resistance parameter equation of the vertical excavation of the drilling mechanism was obtained, providing mechanical parameters and a theoretical basis for the mechanism design of this key component. Wang Kaiyuan et al. [9] used RecurDyn and EDEM software to simulate the hole-forming process of the duck bill hole-forming device at different angles, selecting the optimaangle by comparing the number of soil particles entering the device. Yuan Xiaoliang et al. [10] simulated the process of planting into soil using a two-way coupling simulation. They analyzed the influence of different working parameters on soil particle disturbance and cavitation effect, and cavitation effect and obtained the optimal parameter combination through Box-Behnken test method. Shi Linrong et al. [11] investigated the impact of soil conditions, the form and structure size of hole-forming device on soil entry resistance through rapid shear test and simulation model establishment. While these researchers have made progress in the field of hole-forming processes,, they have not addressed the issue of increasing hole-forming time under high-speed operation conditions, nor have solved the problem of insufficient hole-forming time for cotton dibbler at hight speeds

In summary, the current working speed of the dibbler is generally 3~4 km/h. If the speed is further improved, the quality of the work will be significantly reduced. In view of the above problems, this paper adopts the extended hole-forming method (delayed hole-forming), and designs a new type of crawler-type delayed hole-forming mechanism, which extends the duck bill belt horizontally. The duck bill is changed from the original circular distribution around the duck bill belt to the straight edge elliptical distribution. The original hole-forming device only moves the duck bill at the tangent position to the ground to compress the seed into a hole, and the duck bill is kept open in the whole straight edge after extension, so as to achieve the effect of delayed hole-forming. In this paper, the multi-body dynamics-discrete element coupling model is established by means of EDEM-Recurdyn coupling numerical simulation, orthogonal test and bench test. The interaction mechanism between mechanism and soil in the process of delayed hole-forming is explored, and the key parameters affecting the quality of hole forming are obtained. The working performance of the crawler-type delayed hole-forming mechanism is improved by optimizing the main structural parameters of the delayed hole-forming device, and the optimal parameter combination after the

 doi:10.20944/preprints202406.0097.v1

operation speed is improved is obtained by the box-behnken test. The prototype was made and the working performance of the delayed hole-forming mechanism was verified by the soil tank bench test. Finally, under the premise of ensuring high hole-forming quality, the cotton hole sowing speed was increased to 6km/h. In order to provide a reference for the study of delaying the formation of holes to increase the time of seed dropping and improve the speed of hole sowing on cotton film.

2. Crawler-Type Time-Delay Hole-Forming Device and Working Principle

2.1. Device Structure

The overall structure of the crawler-type time-delay hole-forming device is shown in Figure 1. The hole-forming device is mainly composed of seeding wheel, auxiliary wheel, shock absorber, profiling four-bar linkage mechanism, crawler block, broken film duck bill and other key components.

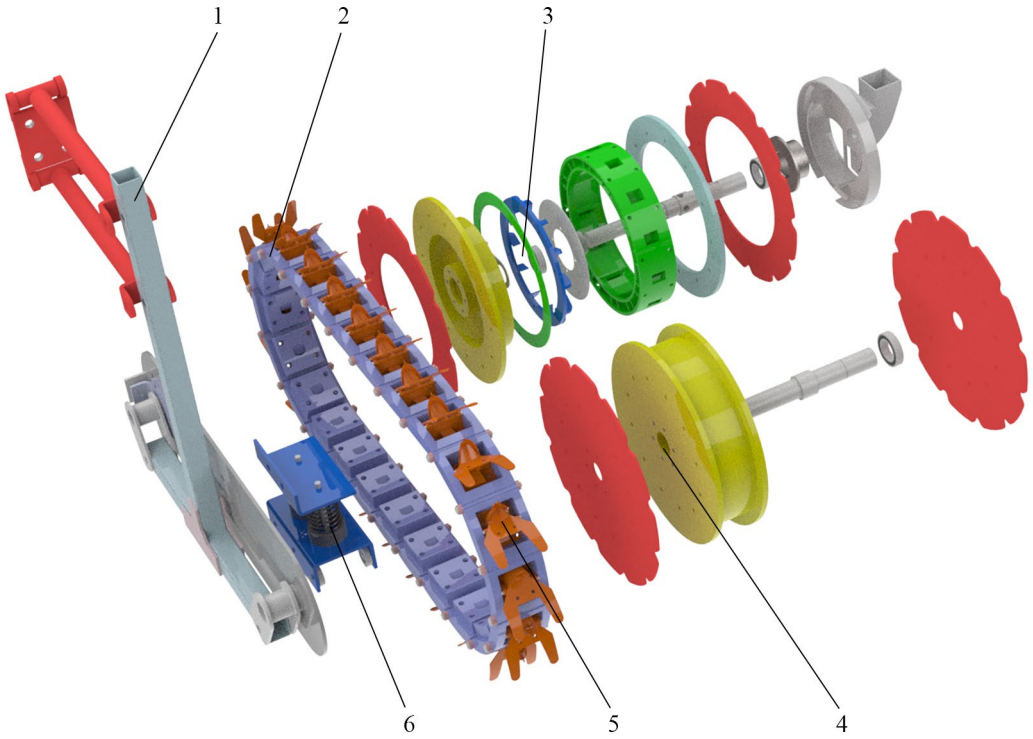

Figure 1. Structure diagram of crawler type delay-time hole-forming device. 1. Profiling four-bar linkage mechanism 2. Crawler block 3. Seeding wheel 4. Auxiliary wheel 5. Broken film duck bill 6. Shock absorber.

2.2. Working Principle

The seed wheel and the auxiliary wheel are installed before and after the meshing sprocket, which is meshed with the copper sleeves on both sides of the connecting pins of each track block. The duck bill is installed on the inner side of the track block, and extends with the track block to achieve the effect of delayed hole formation. Before and after the connecting shaft, each is equipped with a top wire to play a fixed role. The adjusting plate can move left and right along the horizontal position at the same time as the fixed seeding wheel, so as to adjust the distance between the two wheels to realize the track tensioning. One end of the shock absorber is fixed with the positioning plate, and the other end is in contact with the bearing of the crawler block. Under the action of the damping spring, the duck bill is pressed to keep it in the soil all the time. The four-bar linkage mechanism connects the whole machine with the frame, and the upper and lower positions can be adjusted according to the field situation.

As shown in Figure 2, in the working state, the frame is fixed with the tractor and drags the whole machine forward. Under the action of the lateral shear force of the soil on the duck bill and the

 doi:10.20944/preprints202406.0097.v1

ground friction, the crawler rotates, driving the seeding wheel and the auxiliary wheel to rotate synchronously. The duck bill is always in a closed state before contact with the soil. When the spring is rotated to the position of the seeding wheel and the ground tangent point, the duck bill is gradually compressed and opened. From the seeding wheel and the ground tangent point to the auxiliary wheel and the ground tangent point, the duck bill is always kept open to achieve the delayed hole-forming effect. After leaving the cutting point of the auxiliary wheel, the ground pressure gradually decreases, and the moving duck bill is closed and works circularly.

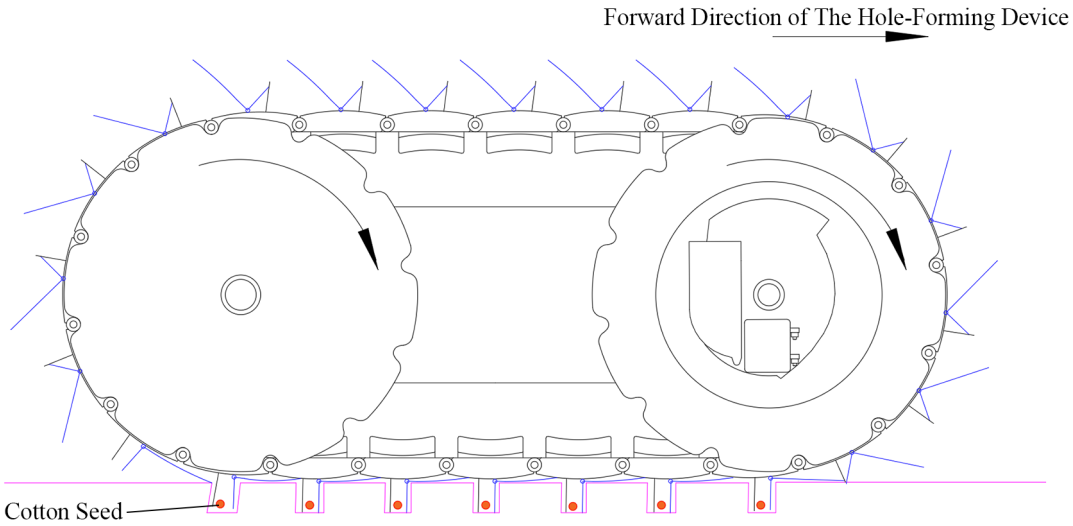

Figure 2. Working principle diagram of the hole-forming device.

2.3. Structural Design of Critical Component

The membrane-breaking duck bill device and the connecting track are the key components to realize the crawler-type time-delayed hole-forming device. Its structure and parameters directly affect the time-delayed hole-forming effect and high-speed seeding quality. Therefore, according to the fact that the diameter of the commonly used metering wheel on the market is generally between 350 mm and 420 mm, the previous research of the project team and only the semicircle of the auxiliary wheel and the metering wheel is wrapped by the crawler, the diameter of the corresponding metering wheel and the auxiliary wheel of the device is set to 370 mm. According to the agronomic requirements and the common size of the current cotton dibbler, the cotton plant spacing was selected as 100 mm according to the reference [12–14]. It can be seen from Figure 2 that the number of duck bill that the track always contacts with the ground is 7, and the contact length between the track and the ground during the operation of the machine is always 700 mm. In summary, the track length is 2362 mm.

In the film-breaking duck bill device (as shown in Figure 3), the fixed duck bill inclination angle affects the soil entry performance of the hole-forming device, whether the film is picked up when it is unearthed, and the amount of soil moving when it is unearthed [15]. According to the relevant literature, the fixed the tilt angle of the duck bill(α) is initially set in the range of 0~15°. The duck bill hole depth into the soil directly affects the sowing depth of cotton seeds. According to the above-mentioned agronomic requirements of cotton bunch planting, the sowing depth of cotton is generally between 20~30 mm. Considering that the soil surface is not smooth and the duck bill can't be completely inserted into the soil, the project team calculated the depth of the duck bill hole-forming into the soil(h) range of 30~45 mm by the sowing depth, the duck bill inclination angle and the coefficient of variation, as shown in Figure 4.

 doi:10.20944/preprints202406.0097.v1

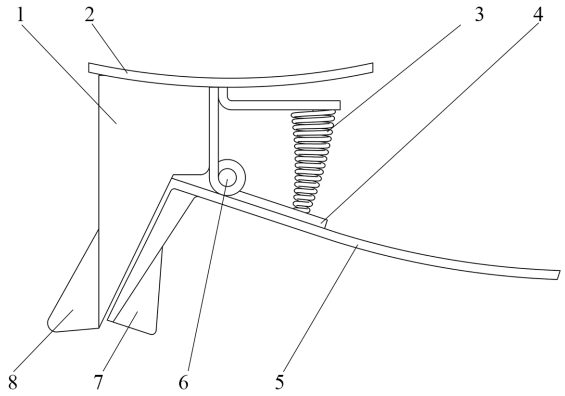

Figure 3. Broken film duck bill structure diagram. 1. Duck bill mounting plate 2. Duck bill fixed mouth 3. Spring 4. Connecting plate 5. Duck bill move mouth 6. Fix stopper 7. Fixed blade 8. Breaking film blade.

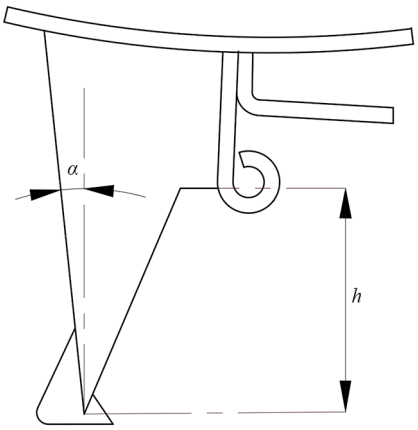

Figure 4. Duck bill fixed bill structure diagram.

The angle of rotation of the moving duck bill(β) affects the distance between the end of the moving duck bill and the end of the fixed duck bill after the duck bill moves to the lowest point. It is a key parameter affecting the quality of cotton seed falling and determines the final emergence effect of cotton seed. If the turning angle is too small, the distance between the opening of the duck bill and the short seed is not enough to fall from the duck bill. If the turning angle is too large, the height difference between the end of the fixed duck bill and the end of the moving duck bill increases, and the soil is easy to fall into the seed hole from the gap of the duck bill, and the position of cotton seed falling is not fixed. Referring to the size of the existing duck bill and the length of the fixed mouth into the soil, the range of the rotation angle of the moving duck bill is set to 24~36°, and the schematic diagram of the rotation of the moving duck bill is shown in Figure 5.

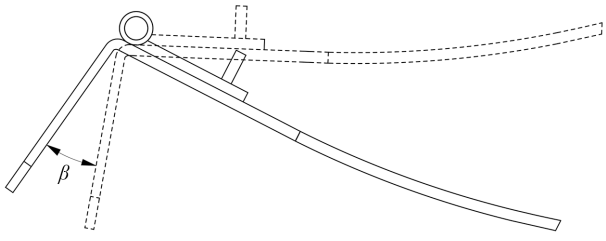

Figure 5. Moving duck bill rotation schematic diagram.

 doi:10.20944/preprints202406.0097.v1

3. Materials and Methods

3.1. Simulation Model Creation and Parameter Setting

The hole-forming effect of the crawler dibbler in the working process is affected by the soil discrete particle system and its own multi-body dynamics system, and the soil particles have certain randomness. It is difficult to accurately evaluate the hole-forming effect of the mechanism only by mathematical model. For this reason, software-assisted calculation is used to verify the rationality of the model.

Discrete Element Method (DEM) and Model based definition (MBD) have been widely used in the field of agricultural machinery in recent years [16–22]. In the process of hole formation, the soil particles are squeezed by the duck bill, and the soil particles collide with each other to form a seed hole, which needs to be analyzed by discrete element method. The duck bill is opened and closed circularly under the action of soil pressure during the working process, and the track block is rotated circularly under the action of sprocket, which needs to be analyzed by multi-body dynamics. The hole-forming effect of the crawler dibbler in the working process is affected by the soil discrete particle system and its own multi-body dynamics system. It is difficult to accurately calculate the hole-forming effect of the mechanism only by mathematical model or single software. In order to observe the movement state of soil in the process of hole formation intuitively and effectively by using DEM-MBD two-way coupling method. In the process of coupling calculation, the multi-body dynamics software initially determines the motion state of the coupling component over time and synchronizes it to the discrete element software. In the discrete element software, the force of the soil particles on the rigid body of the hole-forming mechanism is fed back in real time, and the data is transmitted to the multi-body dynamics model for iterative solution, so as to change the kinematic data of the coupling components and make the simulation results closer to the actual physical behavior. Through this two-way data transmission and in-depth analysis, the interaction mechanism between soil particles and hole formation mechanism can be analyzed more comprehensively. The coupling process and principle are shown in Figure 6.

Preprints.org (www.preprints.org) | NOT PEER-REVIEWED | Posted: 3 June 2024 doi:10.20944/preprints202406.0097.v1

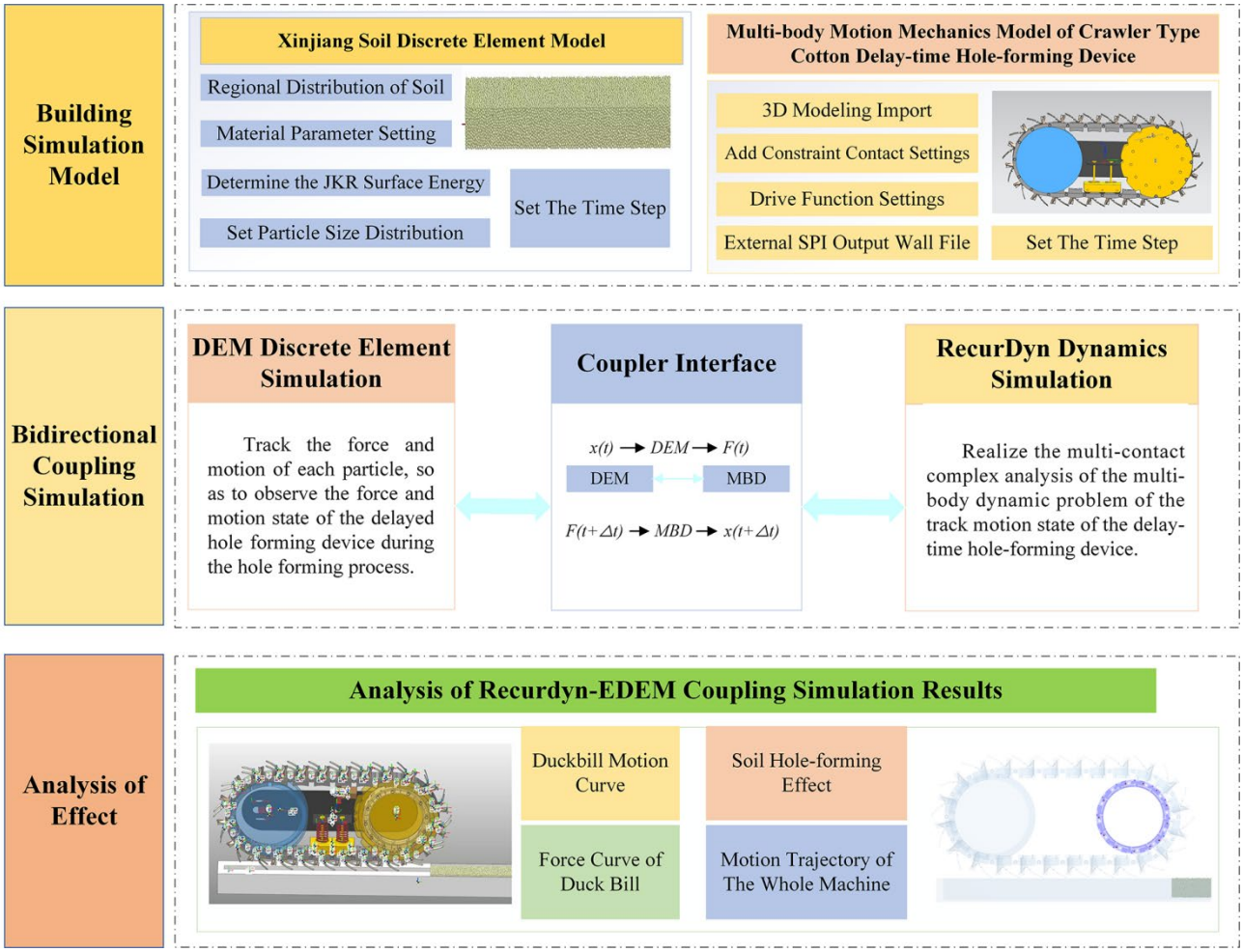

Figure 6. DEM-MBD coupling simulation process and schematic diagram.

After completing the modeling and assembly of the crawler-type hole-forming mechanism in Soildworks, the assembly is converted into stp format and imported into Recurdyn for dynamic simulation of the whole machine. Simplify the three-dimensional model by retaining only the transmission parts and the parts in contact with the soil, omitting other parts. The properties of the track material are set as resin, the seeding wheel and the auxiliary wheel are aluminum alloy, and the support plate, the tensioning wheel mechanism and the duck bill are steel. Determine the density, Young 's modulus, Poisson 's ratio and other parameters.

During the working process of the crawler-type hole-forming mechanism, the positioning plate moves horizontally under the action of traction, and the crawler block rotates and engages with the sprocket. When the duck bill in the crawler block contacts with the soil, it opens and closes when it leaves the soil. In order to realize the above motion process, the motion pair is added to the whole machine structure. Rotary pairs are added between each track block, between the track block and the tensioning wheel, between the fixed mouth and the moving mouth of the duck bill, and between the seeding wheel, the auxiliary wheel and the positioning plate. Tension wheel and tension mechanism mounting plate, the road relative to the coordinate system to add a fixed pair. The profiling four-link phase moves vertically with the coordinate system, and the positioning plate adds a moving pair to the road surface. The virtual prototype after constraint is shown in Figure 7.

Preprints.org (www.preprints.org) | NOT PEER-REVIEWED | Posted: 3 June 2024 doi:10.20944/preprints202406.0097.v1

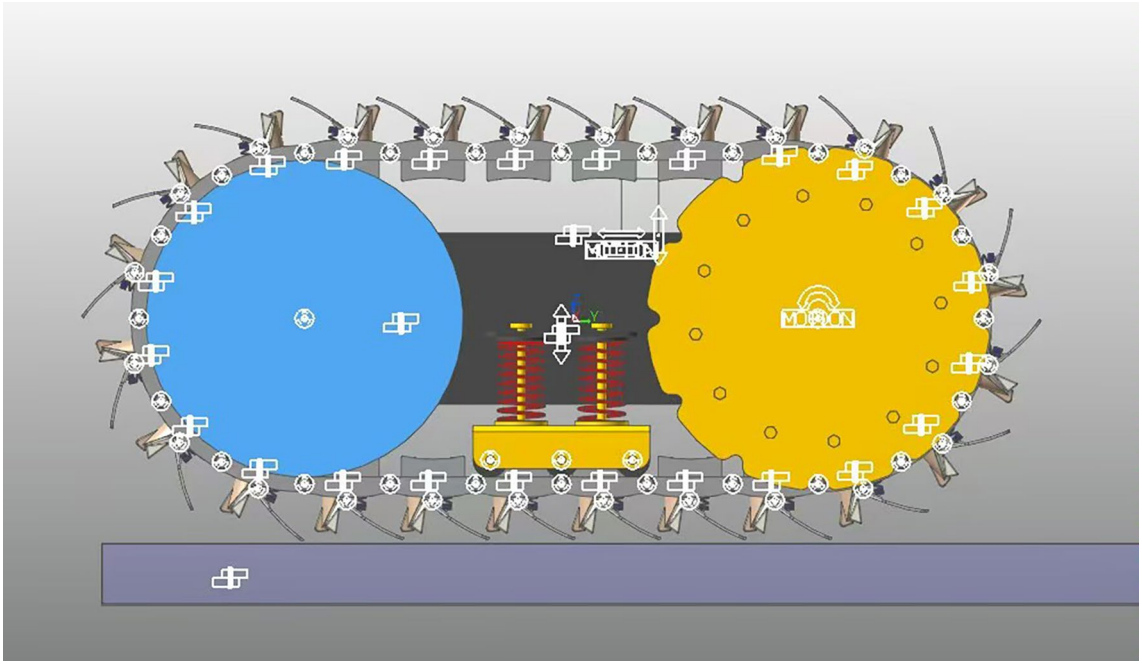

Figure 7. Schematic diagram of the virtual prototype after the constraint of the hole-forming device.

Based on the material characteristics, the bearing of the track block and the seeding wheel, the auxiliary wheel and the tensioning mechanism are determined. Moving duck bill and fixed duck bill; the contact between the moving duck beak and the crawler block. The Hertz contact theory formula studies the local stress and strain distribution of two objects after contact, which is determined by the shape and material properties of the contact object. In the numerical simulation, RecurDyn allows a certain degree of penetration when the object is in contact. The contact force between the two objects is simulated by the elastic coefficient K and the penetration. The elastic coefficient K is determined by the elastic modulus E_1 and E_2 of the two contact materials, the contact radius R_1 and R_2, and the Poisson's ratio. When the actual contact occurs, the RecurDyn contact force is calculated as follow:

$$F = K \cdot \delta^{\frac{3}{2}} \tag{1}$$

$$K = \sqrt{\frac{16RE^2}{9}} \tag{2}$$

$$R = \frac{R_1 R_2}{R_1 + R_2} \tag{3}$$

$$E = \frac{E_1 E_2}{E_2(1-v_1^2) + E_1(1-v_2^2)} \tag{4}$$

$$f_n = f_{ns} + f_{nd} \tag{5}$$

$$f_{ns} = K \cdot \delta^{\frac{3}{2}} \tag{6}$$

$$f_{nd} = step(\delta, 0, \delta_{\max}, C_{\max}) \cdot \dot{\delta} \tag{7}$$

 doi:10.20944/preprints202406.0097.v1

where f_n is formal forc (N), f_{ns} is stiffness forc (N), f_{nd} is damping force, (N), δ is penetratio (mm), C is damping coefficient, N·s/mm.

In order to establish a perfect discrete element contact model of soil particles. The soil physical parameters were measured to determine the soil density of 1.565 g/cm^3, the soil moisture content of 18.3 %, and the soil accumulation angle of 39.6 °. The contact mechanics parameters such as soil JKR surface energy, collision recovery coefficient and dynamic friction are usually unable to be measured directly, and the setting of the above parameters varies greatly in different literatures [24–26]. The above parameters directly determine the degree of adhesion between the particles of the soil model and the trajectory of the particles after the mechanical collision. Therefore, the specific values of the above contact mechanical parameters are obtained by the simulation calibration method with the soil accumulation angle as the standard. Finally, the surface energy of soil JKR was determined to be 6.06 J/m^2, the rolling friction coefficient was 0.15, and the collision recovery coefficient was 0.36. Table 1 shows the design soil parameters.

Table 1. Parameters of soil discrete element simulation model.

Serial Number	Parameter Name	Numerical Value
1	Poisson's ratio of soil particles	0.35
2	Soil particle density (kg/m^3)	1565
3	Soil particle shear modulus (Pa)	1.09×10^6
4	Poisson's ratio of duck bill (steel)	0.3
5	Duck bill (steel) density (kg/m^3)	7865
6	duck bill shear modulus (Pa)	7.9×10^{10}
7	Collision recovery coefficient between soil particles and soil particles	0.36
8	Static friction coefficient between soil particles and soil particles	0.56
9	Rolling friction coefficient between soil particles and soil particles	0.15
10	JKR surface energy of soil particles and soil particles	6.06
11	Collision recovery coefficient between soil particles and duck bill	0.30
12	Static friction coefficient between soil particles and duck bill	0.30
13	Rolling friction coefficient between soil particles and duck bill	3.16

There is an obvious adhesion phenomenon between soil particles in Xinjiang sowing soil. In this study, JKR V2 model is used, which can better reflect the mechanical properties of viscoelastic deformation of adhesive particles. Therefore, compared with the JKR model, it produces a more accurate force calculation. In addition, the study also considers the force effect in the separation process of the adhesion effect between particles. The force-overlap response of the JKR model is shown in Figure 8. When two elastic and viscous spheres are close to each other, the force acting on the sphere is zero (from A to B). When the two spheres have physical contact (B), the DEM contact between the spheres is established, and the normal contact force decreases immediately (C). In the recovery phase, the stored elastic energy is released and converted into kinetic energy, causing the sphere to move in the opposite direction. When the contact overlap becomes zero (C), all the work done in the loading stage is restored. However, the spheres still adhere to each other, and further work is needed to separate the two spheres. In order to disconnect the contact, a minimum force equal to the breaking force (E) is required, and the contact is disconnected at F.

Preprints.org (www.preprints.org) | NOT PEER-REVIEWED | Posted: 3 June 2024 doi:10.20944/preprints202406.0097.v1

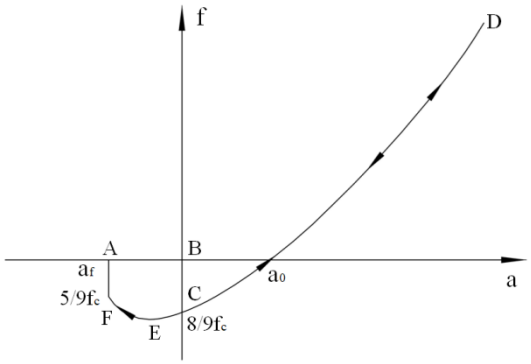

Figure 8. Schematic diagram of the force between the spheres of JKR V2 model.

In order to calculate the adhesion, the $EDEM_r$ needs to be activated and set to be greater than the physical radius of the particle. The calculation formula is as follows:

$$EDEM_r \geq r + \alpha_f \tag{8}$$

where $EDEM_r$ is the contact radius of EDEM (mm), r is the physical radius of particles (mm), α_f is the relative distance of contact fracture, (mm).

The normal contact force in the JKRV2 model is calculated as follows:

$$F_n = \frac{4E\alpha^3}{3R} - \left(8\pi\Gamma E\alpha^3\right)^{\frac{1}{2}} \tag{9}$$

$$\Gamma = \gamma_1 + \gamma_2 - \gamma_{12} \tag{10}$$

$$\alpha_f = \left(\frac{3F_{nc}^{2\ 3}}{16RE^2}\right)^{\frac{1}{3}} \tag{11}$$

where R is the relative radius (mm), Γ is the surface energy (J), γ_1 and γ_2 are the surface energy of two spheres (J), γ_{12} is the contact surface energy. For the special case of contact between two spheres of the same material, γ_{12} is 0, and the interface surface energy becomes Γ is 2γ.

The maximum normal gap δ_c and the maximum adhesion F_{nc} of the particles in the calculation interval are as follows:

$$\delta_c = \frac{\alpha^2}{R} - \left(\frac{2\pi\Gamma\alpha}{E}\right)^{\frac{1}{2}} \tag{12}$$

$$F_{nc} = \frac{3}{2}\pi R\Gamma \tag{13}$$

3.2. Bidirectional Coupling MBD and DEM Simulation Test Scheme and Method

At the initial position of the simulation, the duck bill is in a closed state. A certain gap between the ground and the fixed duck bill is retained to prevent penetration in the initial state model, and the contact force is generated to change the position of the mechanism. In order to make the movement closer to the actual situation, a moving pair moving up and down relative to the Ground is added to the simplified four-bar linkage, and a moving pair moving left and right relative to the

 doi:10.20944/preprints202406.0097.v1

four-bar linkage is added to the simplified rear tube, and the square tube is fixed with the positioning plate. Therefore, the whole machine can only move along the plane with four degrees of freedom. The square tube moving pair is defined along the vertical direction, and the displacement Motions function is step (time, 0, 0, 0.1, -50.5). The four-link moving pair is defined along the horizontal direction, and the velocity Motions function is IF (time-0.2 : 0, 0, 1666.7). That is, the moving speed of the whole machine is 0 before 0.2 s, and the displacement of the whole machine along the negative direction of the z-axis is 50.5 mm in the vertical downward direction at 0.1 s. After the displacement, it contacts with the ground, and the duck bill opens and stabilizes for 0.1 s. After 0.2 s, the four-bar linkage moves horizontally to the right along the positive direction of the y-axis at a speed of 1666.7 mm/s or 6.0 km/h. Under the action of friction, the duck bill drives the track block to rotate, and then drives the seeding wheel to rotate synchronously, and the hole-forming mechanism begins to work.

The Geometry imported by the wall file in the EDEM simulation phase is always consistent with the Body motion process in RecurDyn. After the whole machine is stable in contact with the road surface, it gradually moves to the soil trough EDEM particle group. At this time, the duck bill is inserted into the soil in turn, and the spring compresses the duck bill mouth to open to form a seed hole. The contact information, mechanism force and motion trajectory of the whole machine are determined by the parameters set by RecurDyn and EDEM. The process of the whole machine into the soil is shown in Figure 9.

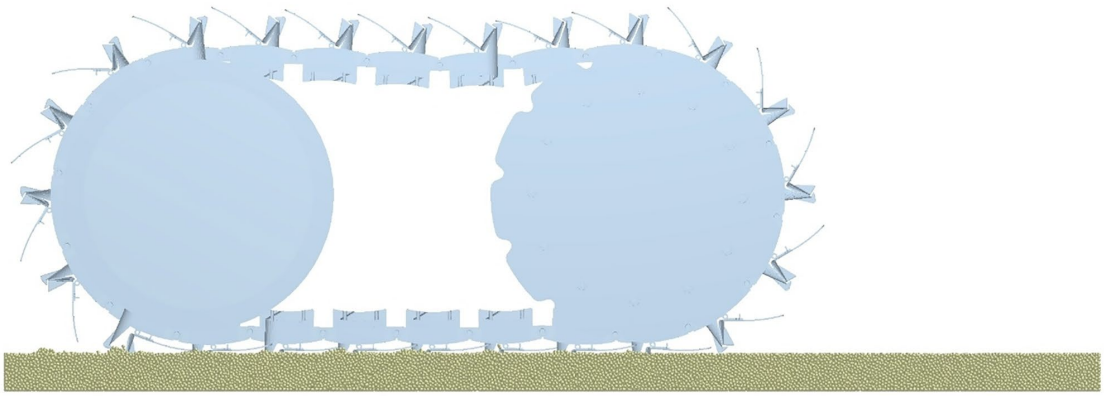

Figure 9. Schematic diagram of the whole process of the hole-forming machine into the soil.

In order to visually display the motion trajectory of the duck bill and the working stability of the whole machine, Marker points are added at the end of the fixed duck bill and the end of the moving duck respectively, and the motion trajectories are displayed with red and black lines respectively. Marker points are added to the centroid of the positioning plate, and the trajectory is displayed in blue lines. It can be seen from Figure 10 that the trajectory of the duck bill can be divided into three sections.

P1P2 section: Before P1 point, the whole machine advanced vertical decline, static and stable for a period of time after contact with the soil, so the duck bill and the fixed mouth trajectory before P1 point is a vertical downward straight line. The red line coincides with the black line. At this stage, the duck bill rotates to contact with the soil. Before contact, the duck bill closes under the action of spring.

P2P3 section: The red line is separated from the black line and has the maximum distance at the end of the trajectory. At this stage, the duck bill enters the soil, and under the action of soil pressure, the duck bill gradually opens and remains open during the extension period. In the process of duck bill leaving the soil, the moving beak swallow tail is fitted with the track block, and the duck bill remains open.

P3P4 section: The red line and the black line gradually coincide. At this stage, the duck bill gradually leaves the soil, the pressure of the spring is reduced, and the duck bill gradually closes. The overall trajectory is a trochoid, and the trajectory coincides and enters the next motion cycle.

 doi:10.20944/preprints202406.0097.v1

The whole stage of the blue line has been a smooth straight line, indicating that the whole machine is stable.

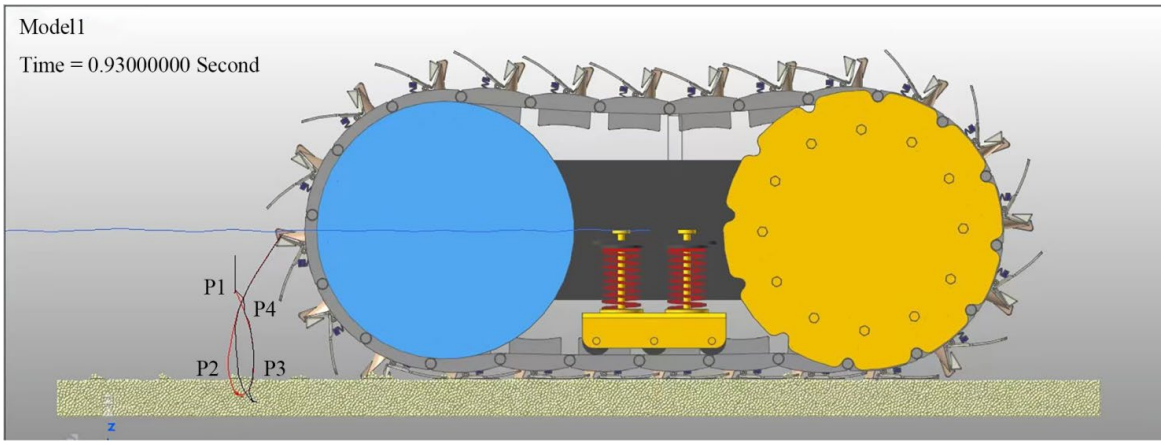

Figure 10. Schematic diagram of the coupled motion trajectory of the hole-forming device.

In order to better analyze the trajectory of the duck bill changing with time, the motion curve of the end of the fixed duck bill and the end of the moving duck bill is derived in RecurDyn Plot, and the two are subtracted to obtain the curve of the opening distance of the duck bill changing with time as shown in Figure 11.

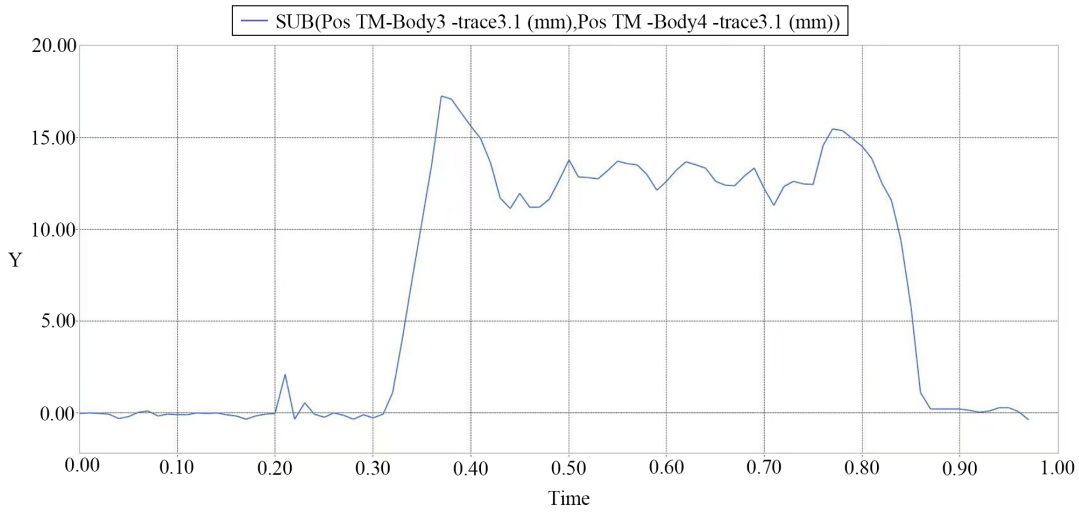

Figure 11. The change diagram of the distance between the end of the fixed duck bill and the end of the moving duck bill during the operation.

As shown in the diagram, before 0.30 s, the duck bill is closed, and the opening distance of the duck bill is 0 mm. After 0.32 s, the duck bill was gradually opened by soil pressure, reaching a maximum of 15.6 mm at 0.36 s, and then decreased slightly to maintain a fluctuation of about 14 mm. Because the dovetail and the crawler block change from fitting with the crawler block to contacting with the crawler block at the end during the extension period, the opening degree is reduced, and under the action of the spring of the damping mechanism, the dovetail has a certain degree of up and down vibration. At 0.76 s, the opening distance is as large as 15.2 mm, and then gradually decreases to 0 and remains unchanged. It can be seen that the opening time of the duck bill is extended to 0.46 s, which provides sufficient time for the falling of cotton seeds. The opening distance of duck bill was 13.4~15.6 mm, which was consistent with the calculated optimal opening value. The above simulation results show that the hole-forming mechanism has high feasibility in the performance of delaying hole-forming and increasing seed-dropping time.

 doi:10.20944/preprints202406.0097.v1

3.2.1. Single Factor Simulation Test

The forward speed of the simulation machine is set to 6 km/h. The soil particles have typical discreteness, and the soil particles change dynamically when they interact with the duck bill, so the quality of the hole changes accordingly after the speed is increased. Therefore, the size of the duck bill structure was adjusted to ensure the quality of the hole-formation. Referring to the structural parameters of the key components and the analysis of the cavitation trajectory of the mechanism, The fixed the tilt angle of the duck bill α, the depth of the duck bill hole-forming into the soil h and the angle of rotation of the moving duck bill β are selected as the experimental factors to carry out the simulation test.

The size of the hole includes the transverse size of the hole, the longitudinal size of the hole and the depth of the hole. The transverse size of the hole is consistent with the width of the duck 's beak, and the value is relatively fixed [27]. Therefore, the evaluation of the effect of the hole is mainly through the EDEM post-processing to measure the effective depth of the hole and the longitudinal length of the hole. The smaller the size of the hole is, the less the evaporation of water in the soil is, and the smaller the size of the hole is, which is conducive to warming and preserving moisture.

The influence of the inclination angle of the fixed duck bill on the quality of the hole is selected. The depth of the duck bill hole-forming into the soil is h = 40 mm, the middle value of the angle of rotation of the moving duck bill is β = 32 °, and the fixed the tilt angle of the duck bill is α = 0 °, 5 °, 10 °, 15 °. The position of soil particles changes in real time during the process of hole formation. In order to more intuitively observe the movement law of soil particles after duck bill extrusion, the longitudinal length of the hole and the depth of the hole were recorded, and the soil particles were not refluxed. In the EDEM post-processing interface, the 'Geometry Bin' function is used to divide the soil into five regions along the vertical soil direction. In 'Particle Seletions', different colors were added to soil particles in different regions, and the color remained unchanged after the position of particles in the same region was changed. The results are shown in Figure 12. The 'Clipping' tool was added to cut the soil from the vertical surface to a 10 mm soil layer along the center line, so as to observe the effect of the hole.

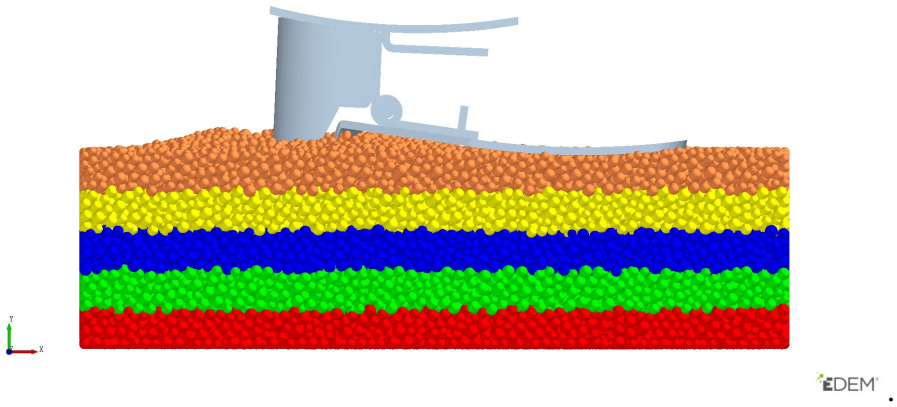

Figure 12. Layered hole-forming effect diagram.

The effect of hole formation under different fixed duck bill inclination angles is shown in Figure 13. The post-processing 'Ruler' tool was used to measure the longitudinal length of the seed hole and the depth of the seed hole after the duck bill left the soil. From the diagram, it can be seen that the longitudinal length of the seed hole increases with the increase of the fixed duck bill inclination angle, and the depth of the seed hole increases first and then decreases with the increase of the fixed duck bill inclination angle. The reason is that the inclination angle of the duck bill increases, the contact time with the soil during the formation of the duck bill is long, and the amount of soil on the side wall of the duck bill is large, so the longitudinal length of the seed hole increases. When the inclination angle of the fixed duck bill is small or large, the extrusion of the soil by the fixed or moving duck bill

 doi:10.20944/preprints202406.0097.v1

is more obvious, the soil particles tend to accumulate to one side, the edge height of the seed hole increases, and the depth of the seed hole increases. Considering the soil disturbance and the effect of hole formation, the duck bill inclination angles of 0 °, 5 °and 10 ° were selected for the subsequent orthogonal test.

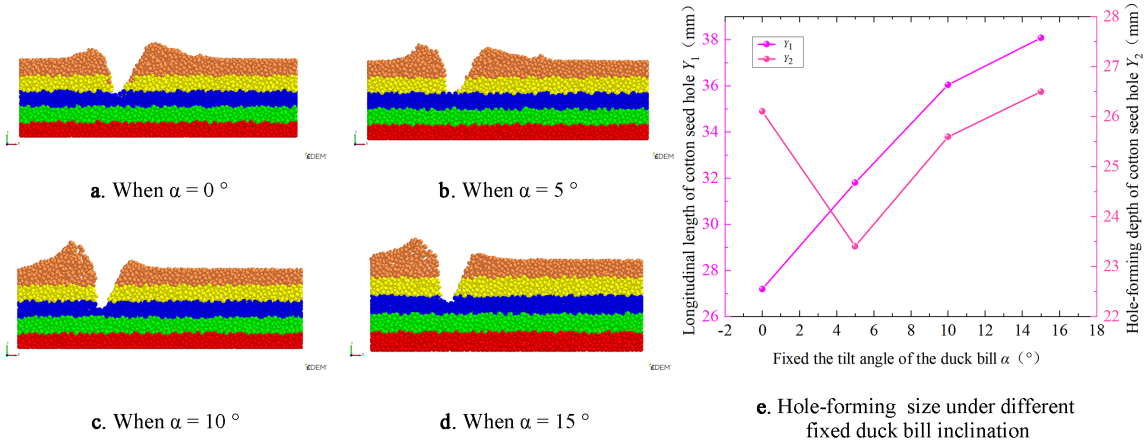

Figure 13. The effect of hole formation under different fixed duck bill inclination angles.

The influence of the depth of the duck bill hole-forming into the soil on the quality of the hole was selected, and the intermediate value of the fixed the tilt angle of the duck bill $\alpha = 5$ ° was selected. The middle value of the angle of rotation of the moving duck bill is $\beta = 32$ °, the depth of the duck bill hole-forming into the soil is h =30mm, 35mm, 40mm, 45mm. The influence of the depth of the duck bill hole-forming into the soil on the effect of hole formation was analyzed. The longitudinal length and effective depth of the seed hole were measured. The change of the effect of the hole with the depth of the duck bill is shown in Figure 14.

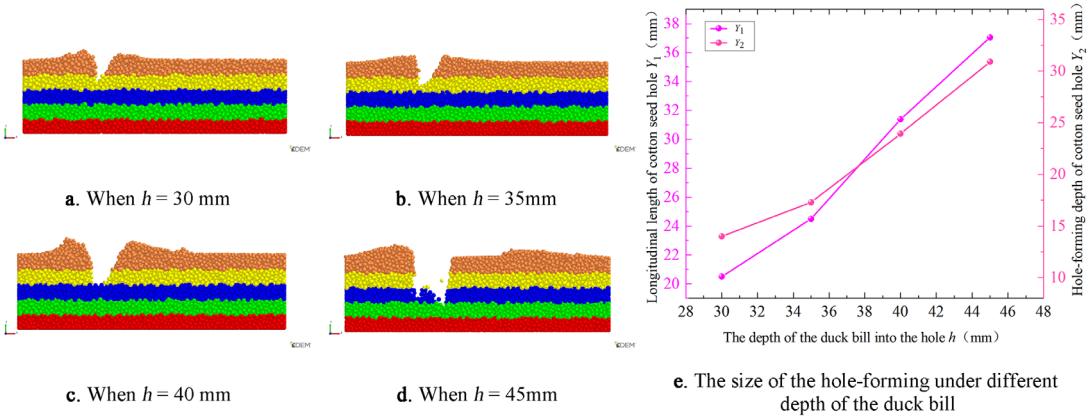

Figure 14. The effect of hole formation under different the depth of the duck bill hole-forming into the soil.

It can be seen from the figure that as the depth of the duck bill increases, the contact area and contact time between the duck bill wall and the soil particles increase, and the longitudinal length and depth of the hole after the duck bill leaves the soil increase. Considering the soil disturbance and the effect of hole formation, the duck bill depth of 35 mm, 40 mm and 45 mm was selected for the subsequent orthogonal test.

The influence of the rotation angle of the moving duck bill on the quality of the hole is selected, and the median value of the inclination angle of the fixed duck bill is $\alpha = 5$ °. The depth of the duck bill hole-forming into the soil is h =40mm., and the angle of rotation of the moving duck bill is β = 24 °, 28 °, 32 °, 36 °. The influence of duck bill rotation angle on soil disturbance was analyzed. The longitudinal length and effective depth of the seed hole were measured. The change of the effect of the hole with the angle of rotation of the moving duck bill is shown in Figure 15.

Preprints.org (www.preprints.org) | NOT PEER-REVIEWED | Posted: 3 June 2024 doi:10.20944/preprints202406.0097.v1

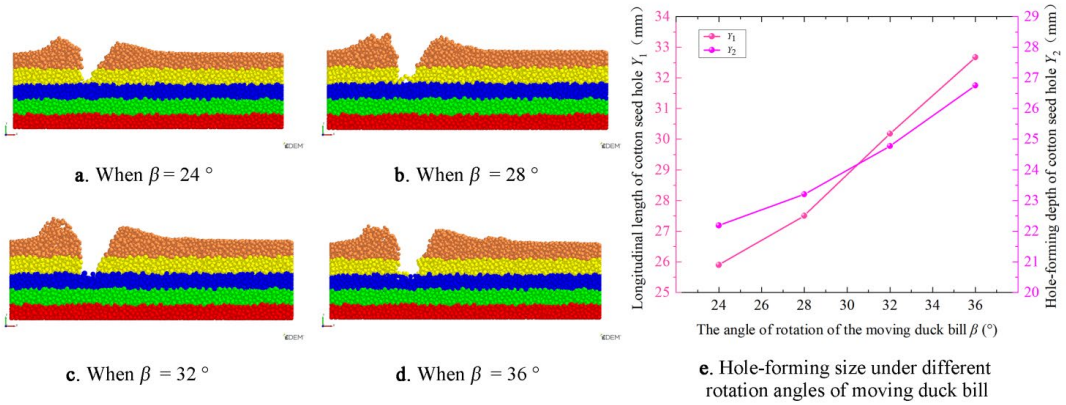

Figure 15. The effect of hole formation under different the angle of rotation of the moving duck bill.

From the diagram, it can be seen that with the increase of the turning angle of the moving duck bill, the longitudinal length of the seed hole and the depth of the hole are increased. The reason is that with the increase of the turning angle of the moving duck bill, the range of the fixed duck bill is unchanged, the degree of rotation of the moving duck bill around the duck bill pin increases, the height difference between the end of the fixed duck bill and the end of the fixed duck bill increases, and the depth of the seed hole increases. At the same time, the soil disturbance near the movable duck bill increases, the soil is enhanced by the shearing and squeezing of the duck bill, and the offset of the soil to the movable duck bill side increases during the hole formation process, resulting in an increase in the longitudinal length. Considering the soil disturbance and the effect of hole formation, the duck bill rotation angles of 28 °, 32 ° and 36 ° were selected for subsequent experiments.

3.2.2. Quadratic Regression Orthogonal Rotation Combination Simulation Test Scheme

In order to further study the influence of The fixed the tilt angle of the duck bill $\alpha(A)$, the depth of the duck bill hole-forming into the soil $h(B)$ and the angle of rotation of the moving duck bill $\beta(C)$ on the working performance of the crawler-type delayed hole formation mechanism. Based on the parameter range determined by the structural parameter design of the key components and the single factor simulation test, the influence of each factor and its interaction on the working performance of the hole formation mechanism is further studied. According to the single factor test of the project team, the value range of each factor is determined, and the experimental design is carried out according to the Box-Benhnken center combination design theory. The level coding of each factor is shown in Table 2. Through the relevant high-level papers and the above single-factor test, longitudinal length of cotton seed hole Y_1 and hole-forming depth of cotton seed hole Y_2 were selected as the experimental hole formation indexes of the effect of the seed hole, and the specific values were measured by EDEM post-processing.

Table 2. Factors and levels of virtual test.

Test factors		Coded value		
		- 1	0	1
A	Fixed the tilt angle of the duck bill (°)	0	5	10
B	The depth of the duck bill into the hole (mm)	35	40	45
C	The angle of rotation of the moving duck bill (°)	28	32	36

3.3. Bench test conditions and methods

It is an important step to further improve the sample to verify the actual operation and the performance of the crawler-type delay hole formation mechanism. This experiment was carried out in the soil trough laboratory. The test was carried out according to the test standards required by JB/T7732-2023 'film seeder' [28] and GB/T6973-2005 'single grain (precision) seeder test method' [29] and high-level papers related to the quality of the hole. The main purpose is to test the working

 doi:10.20944/preprints202406.0097.v1

performance of the crawler delay hole-forming mechanism and the quality of the hole formation operation when the forward speed of the machine is increased to 6 km/h. By comparing the simulation results under the optimal conditions of each factor with the results of the soil trough bench test of the machine. The longitudinal length of cotton seed hole Y_1 and hole-forming depth of cotton seed hole Y_2 were used to evaluate and verify the hole-forming performance of the delayed hole-forming device. Taking the hole dislocation rate H_c and the hole distance qualified rate H_x of the crawler type delay hole forming device as the evaluation standard of the working quality, to judge whether its working performance meets the national standard. At the same time, according to the results of the soil bin verification test, it provides a reference for the subsequent improvement and optimization of the prototype performance.

$$H_c = \frac{c_h}{f} \times 100 \tag{14}$$

$$H_x = \frac{x_h}{f} \times 100 \tag{15}$$

where C_h is the number of misaligned membrane pores, X_h is the qualified number of hole distance, f is the total determination of membrane pore number.

On March 5,2024 in Xinjiang Xin Changsheng Agricultural Machinery Co., Ltd. soil trough bench test, as shown in Figure 16. The soil was leveled by rotary tillage in the early stage, and the soil type was sandy loam. The test soil bin is 150 m long and 10 m wide. The main instruments of the test equipment are: crawler-type cotton time-delay hole-forming device prototype, 2MBJ film laying and soil preparation assembly, high-speed camera, tape, steel ruler, steel swab and so on. Before the test, the 2MBJ film-paving and soil preparation assembly was used to complete the film-paving operation. During the test, the forward speed of the prototype was set to 6km/h, the working parameters of the key components were set to the values under the optimal simulation conditions, and the forward distance was set to 15 m each time. The velocity is not stable in the initial and stop motion stages of the time-delay hole-forming device. Therefore, only the test soil tank selected for the test is composed of three parts: starting area, measuring area and parking area. The length of the test area is 10 m, and the start-up area and parking area are both 2.5 m. Theoretically, 100 holes can be formed in the measurement area (10m).

Figure 16. Prototype of crawler-type time-delay hole-forming device.

4. Results and Discussion

The simulation test results based on the above design scheme are shown in Table 3, including 12 analysis factors and 5 coordinate origin tests for estimating errors. The Design-Expert 13 software was used to perform a quadratic multiple regression fitting analysis on the results of Table 3, and a

 doi:10.20944/preprints202406.0097.v1

regression model between the influencing factors and the evaluation indicators was established (see Formulas 1 and 2 for details).

$$Y_1 = 33.1 + 2.45 * A + 1.7 * B + 2.05 * C - 0.2 * AB - 1.05 * AC + 1.6 * BC - 2.08 * A^2 - 0.33 * B^2 - 0.73 * C^2 \quad (16)$$

$$Y_2 = 27.66 + 1.04 * A + 1.06 * B + 2.03 * C - 1.7 * AB + 0.42 * AC + 0.28 * BC - 1.58 * A^2 - 0.73 * B^2 - 0.5 * C^2 \quad (17)$$

Table 3. Test schemes and results.

Test number	Factors			Longitudinal length of cotton seed hole Y_1 (mm)	Hole-forming depth of cotton seed hole Y_2 (mm)
	A	B	C		
1	- 1	- 1	0	26.2	21.2
2	1	- 1	0	31.3	27.0
3	- 1	1	0	30.5	27.1
4	1	1	0	34.8	26.1
5	- 1	0	- 1	24.3	23.1
6	1	0	- 1	31.5	24.0
7	- 1	0	1	31.2	26.3
8	1	0	1	34.2	28.9
9	0	- 1	- 1	30.5	23.8
10	0	1	- 1	30.2	25.0
11	0	- 1	1	30.7	27.3
12	0	1	1	36.8	29.6
13	0	0	0	32.5	27.9
14	0	0	0	34.2	27.7
15	0	0	0	33.5	27.7
16	0	0	0	32.7	27.1
17	0	0	0	32.6	27.9

4.1. Variance Analysis and Discussion

The regression coefficients in the regression model of the evaluation indexes Y_1 and Y_2 were analyzed by F test and analysis of variance (ANOVA). The results are shown in Table 4. According to the significant value P, $P_{L1} = 0.4887 > 0.05$ and $P_{L2} = 0.3896 > 0.05$ (both are not significant) of the regression model of the objective function Y_1 and Y_2 in Table 4, it shows that the loss of fit of the two models is not significant, and there is no loss factor in the regression analysis. The model has a high degree of fitting with the actual test. The P value of the regression term of the model is extremely significant, $P_{M1} < 0.0001$, $P_{M2} < 0.0001$, indicating that the regression results have certain reliability.

According to ANOVA, the significant value P of each influencing factor in the experiment can be determined. For the evaluation index Y_1, the factors A, B, C, BC and A^2 have a very significant impact, and the factor AC has a significant impact. For the evaluation index Y_2, factors B, C, AC, A^2, B^2 and C^2 have a very significant impact, and factors A and BC have a significant impact. The F value analysis of each factor in Table 4 shows that the larger the F value, the higher the influence of each factor on the test evaluation index. Therefore, the primary and secondary order of the influence of each test factor on the longitudinal length of cotton seed hole Y_1 is: A > C > B. The primary and secondary order of the influence of each test factor on the hole-forming depth of cotton seed hole Y_2 is: B > C > A.

 doi:10.20944/preprints202406.0097.v1

Table 4. ANOVA of regression model.

Indicator	Source of variance	Sum of squares	Freedom	Mean square	*F*	*P*	significant
Y_1	Model	141.62	9	15.74	29.77	< 0.0001	**
	A	48.02	1	48.02	90.85	< 0.0001	**
	B	23.12	1	23.12	43.74	0.0003	**
	C	33.62	1	33.62	63.61	< 0.0001	**
	AB	0.16	1	0.16	0.3	0.5993	
	AC	4.41	1	4.41	8.34	0.0234	*
	BC	10.24	1	10.24	19.37	0.0032	**
	A^2	18.13	1	18.13	34.3	0.0006	**
	B^2	0.44	1	0.44	0.84	0.3895	
	C^2	2.21	1	2.21	4.19	0.08	
	Residual	3.7	7	0.53			
	Lack-of-fit	1.56	3	0.52	0.97	0.4887	*ns*
	Pure Error	2.14	4	0.53			
	Corrected Total	145.32	16				
Y_2	Model	194.15	9	21.57	34.56	< 0.0001	**
	A	7.22	1	7.22	11.57	0.0114	*
	B	67.86	1	67.86	108.71	< 0.0001	**
	C	54.6	1	54.6	87.47	< 0.0001	**
	AB	0.12	1	0.12	0.2	0.6711	
	AC	13.69	1	13.69	21.93	0.0023	**
	BC	5.52	1	5.52	8.85	0.0207	*
	A^2	11.19	1	11.19	17.92	0.0039	**
	B^2	8.91	1	8.91	14.28	0.0069	**
	C^2	20.47	1	20.47	32.8	0.0007	**
	Residual	4.37	7	0.62			
	Lack-of-fit	2.16	3	0.72	1.3	0.3896	*ns*
	Pure Error	2.21	4	0.55			
	Corrected Total	198.52	16				

Note: * indicates significance ($p < 0.05$); ** indicates high significance ($p < 0.01$); *** indicates high significance ($p < 0.001$).

 doi:10.20944/preprints202406.0097.v1

4.2. Interactive Analysis and Discussion

In order to express the interaction effect of various factors on the longitudinal length of cotton seed hole Y_1 and hole-forming depth of cotton seed hole Y_2, the quadratic regression equation of the above two evaluation indexes was reduced. One of the factors was set to the 0 level, and the other two factors were analyzed for interaction effects (removing meaningless interaction items: *AB* interaction with insignificant effects in evaluation indicators Y_1 and Y_2). The influence of *AC* and *BC* interaction on the evaluation indexes Y_1 and Y_2 was studied, and the corresponding response surface was generated.

The response surface graph can well reflect the interaction between independent variables. By observing the steepness of the slope of the response surface diagram, the degree of influence of the two on the response value is determined. The steeper the response surface diagram is, the more obvious the interaction between the two is. The effects of fixed the tilt angle of the duck bill (*A*), the depth of the duck bill into the hole (*B*), the angle of rotation of the moving duck bill (*C*) on the longitudinal length of cotton seed hole Y_1 and hole-forming depth of cotton seed hole Y_2 are shown in Figure 17 and Figure 18.

The effect of the interaction between the fixed the tilt angle of the duck bill (*A*) and the angle of rotation of the moving duck bill (*C*) on the longitudinal length of cotton seed hole Y_1 is shown in Figure 17**b**. In the *AC* interaction surface, when the value of the moving duck bill angle is small, the change slope of the longitudinal length increases first and then flattens out with the increase of the fixed duck bill angle. In the *AC* interaction surface, when the value of the moving duck bill angle is small, the change slope of the longitudinal length increases first and then flattens out with the increase of the fixed duck bill angle. In the AC interaction surface, when the value of the moving duck bill angle is small, the change slope of the longitudinal length increases first and then flattens out with the increase of the fixed duck bill angle. This shows that there is a significant interaction between the fixed duck bill angle and the moving duck bill angle. In the case of only considering the interaction between the two, when the duck bill inclination angle is 0~2 ° and the duck bill rotation angle is about 28~30 °, the longitudinal length Y_1 is smaller.

The effect of the interaction between the depth of the duck bill into the hole (*B*) and the angle of rotation of the moving duck bill (*C*) on the longitudinal length of cotton seed hole Y_1 is shown in Figure 17**c**. In the *BC* interaction surface, when the turning angle of the moving duck bill is small, the longitudinal length tends to be gentle with the increase of the depth of the duck bill into the soil. When the turning angle of the moving duck bill is large, the longitudinal length increases with the increase of the depth of the duck bill into the soil, and the longitudinal length increases with the increase of the turning angle of the moving duck bill. When the depth of the duck bill is different, the longitudinal length varies with the increase of the turning angle of the moving duck bill. This shows that there is a significant interaction between the depth of the duck bill and the turning angle of the moving duck bill. Only considering the interaction between the two, when the depth of the duck bill is 35~37 mm and the turning angle of the moving duck bill is about 28~30 °, the longitudinal length Y_1 is smaller.

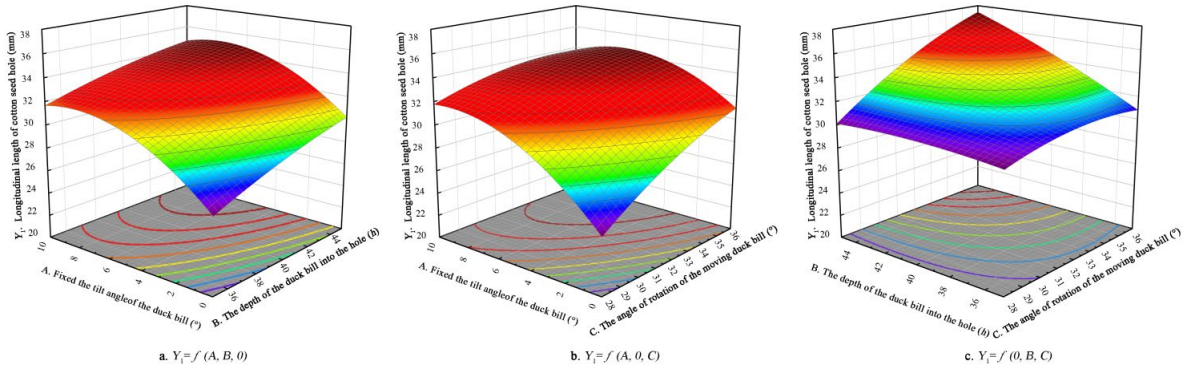

a. $Y_1=f\ (A, B, 0)$ b. $Y_1=f\ (A, 0, C)$ c. $Y_1=f\ (0, B, C)$

Figure 17. The response surface diagram of the interaction of various factors on the longitudinal length of cotton seed hole.

Preprints.org (www.preprints.org) | NOT PEER-REVIEWED | Posted: 3 June 2024 doi:10.20944/preprints202406.0097.v1

The effect of the interaction between the fixed the tilt angle of the duck bill (*A*) and the angle of rotation of the moving duck bill (*C*) on the hole-forming depth of cotton seed hole Y_2 is shown in Figure 18**b**. In the *AC* interaction surface, the change slope of the depth of the hole increases first and then decreases with the increase of the fixed duck bill inclination angle. The slope of the change of the depth of the hole increased with the increase of the angle of the duck bill. In the case of only considering the interaction between the two, it is known that when the duck bill inclination angle is 0~2 ° and the duck bill rotation angle is about 28.8~30 °, the depth of the hole Y_2 is smaller.

The effect of the interaction between the depth of the duck bill into the hole (*B*) and the angle of rotation of the moving duck bill (*C*) on the hole-forming depth of cotton seed hole Y_2 is shown in Figure 18**c**. In the *BC* interaction surface, with the increase of the depth of the duck bill into the soil and the rotation angle of the moving duck bill, the depth of the hole increased slowly. Only considering the interaction between the two, it is known that when the depth of the duck bill is 35~37 mm and the angle of the moving duck bill is about 28.8~30 °, the depth of the hole Y_2 is smaller.

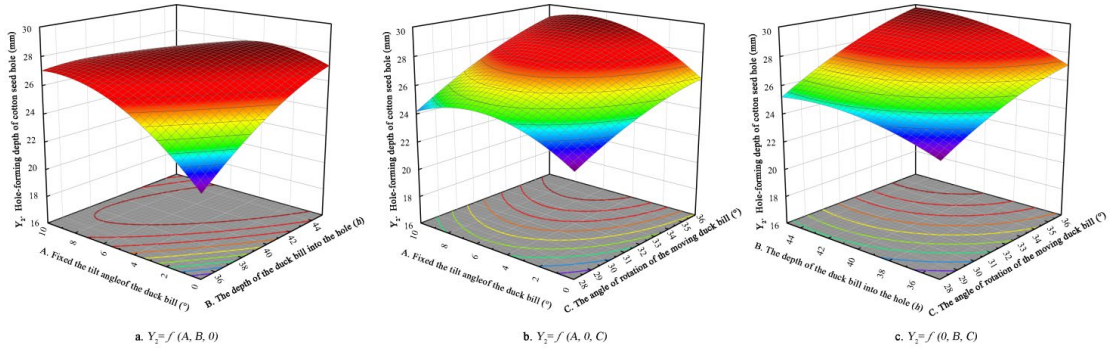

Figure 18. The response surface diagram of the interaction of various factors on the hole-forming depth of cotton seed hole.

4.3. Comprehensive Optimal Design

After the hole-forming operation, the hole size is required to be as small as possible under the premise of ensuring the depth of penetration, so as to facilitate soil moisture conservation, reduce water evaporation, and improve the quality of cotton seed germination. Therefore, according to the regression equation model, the minimum longitudinal length and the target value of the depth of the hole are 25 mm as the optimization objectives. The predicted optimal conditions are as follows: the effects of fixed the tilt angle of the duck bill (*A*) is 2.36 ° , the depth of the duck bill into the hole (*B*) is 42.36 mm, and the angle of rotation of the moving duck bill (*C*) is 30.48 °. According to the actual conditions, the conditions are corrected to be *A* of 2 °, *B* of 42 mm, and *C* of 30 °. The longitudinal length of the corresponding seed hole Y_1 is 26.379 mm, and the depth of the seed hole Y_2 is 25.00 mm. Under this optimal condition, the simulation test of the whole machine is carried out, as shown in Figure 18. The average Y_1 was 27.1 mm, and the error with the optimization result was 2.82 %. The average Y_2 was 24.3 mm, and the error with the optimization result is 2.80 %. All in the 5% range.

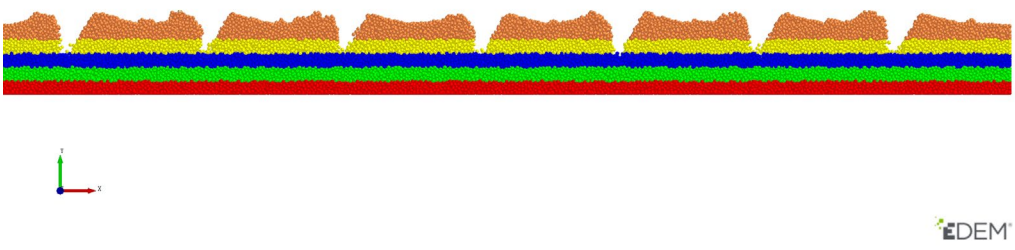

Figure 19. The schematic diagram of the operation effect of the delayed hole-forming device after comprehensive optimization.

 doi:10.20944/preprints202406.0097.v1

4.4. Comparison with The Results of Soil Bin Bench Test

From the previous simulation results, it can be seen that under the optimal conditions (*A* of 2 °, *B* of 42 mm, *C* of 30 °). The Y_1 calculated by the coupling model was 27.1 mm, and the Y_2 was 24.3 mm. The soil trough bench test of the prototype was carried out under the optimal conditions of each factor, as shown in Figure 20. After the operation was completed, the test was divided into five regions according to GB/T6973-2005 [29]. Five seed holes were randomly selected in each region, and the size of the pits after the actual operation was measured. The mean value of each region was used as the final test result. The results are shown in Table 5.

a. Bench Validation Experiments **b**. Effective Depth of Hole Formation **c**. Longitudinal Length of Hole Formation

Figure 20. Bench verification test and schematic diagram of hole-forming effect.

Table 5. Results and comparison of field validation test.

Test	Longitudinal length of cotton seed hole Y_1			Hole-forming depth of cotton seed hole Y_2		
	Simulation value (mm)	Test value (mm)	Relative error (%)	Simulation value (mm)	Test value (mm)	Relative error (%)
1	27.1	29.2	7.58	24.3	23.1	5.18
2		29.0	7.05		25.1	1.99
3		28.0	3.56		22.2	8.76
4		29.4	8.52		22.5	7.56
5		29.7	9.77		23.3	3.98
Average	/	29.1	7.23	/	23.2	4.36

It can be seen from Table 5 that the average longitudinal length of cotton seed hole Y_1 is 29.1 mm, and hole-forming depth of cotton seed hole Y_2 is 23.2 mm. Compared with the results of the previous coupling simulation model, the relative errors of the two are 7.23 % and 4.36 %, respectively. Due to the simplification of some parts of the hole forming mechanism in the RecurDyn-EDEM coupling simulation, and the parameter calibration of the soil has certain errors, the physical parameters of the soil particles fluctuate within a certain range in the actual situation, resulting in the deviation between the simulated soil model and the actual soil model. At the same time, the actual soil is not completely flat compared with the simulation model, resulting in fluctuations in the specific depth of the hole and the rate of penetration.

According to the requirements of JB/T7732-2023 [28], the actual hole distance and the required hole distance of ± 1.5 cm are considered to be qualified, and the film-covered film hole is regarded as the hole dislocation. Three regions with stable velocity were selected for recording and measurement. The calculated hole dislocation rate H_c is 4.33 %, which does not exceed the national standard of 6 %. The qualified rate of hole distance H_x is 94.33 %, higher than the national standard requirement of 80 %.

Adjust the traction speed of the rack to adjust the operating speed of the hole forming mechanism. The opening time of the duck bill at 6 km/h was recorded by a high-speed camera, and

 doi:10.20944/preprints202406.0097.v1

the opening time of the duck bill was recorded as shown in Table 6. From the simulation results, it can be seen that the time required for the cotton seed to fall from the duck bill is 0.11 s, and the opening time of the duck bill of the crawler-type hole-forming device is much longer than the time required for the cotton seed to fall.

Table 6. The opening time of the duck bill at the working speed of 6 km/h of the delay hole-forming device.

Test	duck bill opening time (s)
1	0.45
2	0.46
3	0.44
4	0.46
5	0.45
Average	0.45

In summary, the simulation test and bench test results of the crawler-type delay hole-forming device designed in this paper are within the range of actual operation requirements, and the bench verification test results are basically consistent with the previous RecurDyn-EDEM coupling simulation analysis results of the delay hole-forming device. It shows that the crawler cotton sowing delay hole-forming device based on RecurDyn-EDEM coupling has better working performance, and achieves the goal of delaying hole-forming and increasing falling time when the forward speed of the machine is increased to 6 km/h. It lays a foundation for high-speed and accurate seeding of cotton planter, and can meet the requirements of high-speed seeding of cotton in China. It has certain reference value.

5. Conclusions

Based on the RecurDyn-EDEM coupling simulation method and the new concept of 'delayed hole-forming', a crawler cotton delayed hole-forming device was developed and modeled. The RecurDyn-EDEM model of the developed crawler-type cotton time-lapse hole-forming device was verified by the combination of pre-test, single-factor simulation test, multi-factor virtual simulation test and soil trough bench verification test, and the interaction between the operation parameters and the operation performance of the time-lapse hole-forming device was analyzed. Based on the response surface optimization design, ANOVA and bench verification test, the following conclusions can be drawn.

(1) The order of the primary and secondary factors affecting the longitudinal length of cotton seed hole Y_1 of the time-delay hole-forming device is: the fixed the tilt angle of the duck bill A > the angle of rotation of the moving duck bill C > the depth of the duck bill hole-forming into the soil B. The order of primary and secondary factors affecting the hole-forming depth of cotton seed hole Y_2 of the delayed hole forming device is: $B > C > A$.

(2) The bench verification test results show that under the optimized combination of operating parameters, the average longitudinal length of cotton seed hole Y_1 is 29.1 mm, and the hole-forming depth of cotton seed hole Y_2 is 23.2 mm. Compared with the results of the previous coupled simulation model, the average relative errors of the two are 7.23 % and 4.36 %, respectively, indicating the accuracy and effectiveness of the established DEM simulation model and virtual test analysis.

(3) In the bench verification test, the hole-forming area and the opening time of the duck bill were recorded and measured after the machine ran stably. The calculated hole dislocation rate H_c was 4.33 %, which did not exceed the national standard requirement of 6 %. The qualified rate of hole distance H_x is 94.33 %, which is much higher than the national standard requirement of 80 %. The average opening time of the duck bill at the speed of 6 km/h is 0.45 s, which is much longer than the time required for cotton seeds to fall from the duck bill (The time required is 0.11 s). Which can meet the requirements of high-speed planting of cotton in China.

In this paper, the experimental analysis is only completed in the soil trough laboratory, and the field operation is relatively more complex and changeable. In the follow-up study, field experiments

 doi:10.20944/preprints202406.0097.v1

can be carried out and the relevant parameters of the delay-time hole-forming device can be further optimized according to the test results. At the same time, this paper only carries out simulation analysis and soil bin test verification on the interaction mechanism between the hole-forming device and the soil after the speed is increased. Subsequently, the position and initial velocity of cotton seeds falling from the seed metering device into the duck bill hole-forming device can be determined by calculation or experiment, and the motion trajectory and seeding effect of cotton seeds after delayed hole forming can be analyzed and determined. With the in-depth understanding of the subject and the actual needs of field operations, I believe that the above content will be the focus of future research.

Author Contributions: Conceptualization, F.P., and C.J.; methodology, F.P., B.W. and J.C.; software, F.P., J.C. and X.J.; validation, F.P., C.J. and H.Z.; formal analysis, F.P., B.W. and H.Z.; investigation, F.P. and H.Z.; resources, F.P., B.W. and C.J.; data curation, F.P., X.J. and H.Z.; writing—original draft preparation, F.P.; writing—review and editing, F.P. and C.J.; visualization, F.P. and H.Z.; supervision, C.J.; project administration, F.P., B.W. and C.J.; funding acquisition, C.J. All authors have read and agreed to the published version of the manuscript.

Funding: This research was funded by the National Natural Science Foundation of China (NSFC) (No. 32101634), and the Key Scientific and Technological Projects in Key Areas of the Xinjiang Production and Construction Corps (No. 2023AB038, 2020AB011), and the Young Science and Technology Top Talent Program of Tianshan Talent Training Program in Xinjiang Province.

Institutional Review Board Statement: Not applicable.

Informed Consent Statement: Not applicable.

Data Availability Statement: Data are contained within the article.

Conflicts of Interest: The authors declare no conflicts of interest.

References

1. Wang, Q.Z., E. H.; Li, F. M.; Wang, X. L. Optimum ratio of ridge to furrow for planting potato in micro-water harvesting system in semiarid areas. *Transactions of the CSAE* **2005**, 38-41.
2. Liu, J.G.L., Y. B.; Zhang, W.; Sun, Y. Y. . The Distributing of the Residue Film and Influce on Cotton Growth Under Continuous Cropping in Oasis of Xinjiang. *Journal of Agro-Environment Science* **2010**, *29*, 246-250.
3. Lou, S.W.D., H. Z.; Tian, X. L.; Tian, L. W. The " Short, Dense and Early" Cultivation of Cotton in Xinjiang: History, Current Situation and Prospect. *Scientia Agricultura Sinica* **2021**, *54*, 720-732.
4. Wu, J.S.C., X. G. Present situation, problems and countermeasures of cotton production mechanization development in Xinjiang Production and Construction Corps. *Transactions of the CSAE* **2015**, *31*, 5-10, doi:10.11975/j.issn.1002-6819.2015.18.002.
5. Li, M.M.C., Y. L.; Hu, B.; Chen, X. G.; Li, Y.; Tang, F.;Sun, X. D. Adaptability of Air - suction Melon Precision Metering Mechanism to Different Size Seeds. *Journal of Agricultural Mechanization Research* **2015**, *37*, 179-182, doi:10.13427/j.cnki.njyi.2015.03.044.
6. Tan, X.Z.W., S. G. Structural characteristics and principle analysis of air-suction precision cave planter. *Xinjiang Farm Research of Science and Technology* **2016**, *39*, 35-38.
7. Li, M.W., W. B.; Du, S.; Guo, S. L.; Li, J. H. Experiment study on adsorption accuracy of air suction cotton dibbler. *Journal of Chinese Agricultural Mechanization* **2016**, *37*, 10-13, doi:10.13733/j.jcam.issn.2095-5553.2016.07.003.
8. Xiang, W.W., M. L.; Lü, J. N.; Quan, W.; Ma, L.; Liu J. J. Calibration of simulation physical parameters of clay loam based on soil accumulation test. *Transactions of the CSAE* **2019**, *35*, 116-123, doi:10.11975/j.issn.1002-6819.2019.12.014.
9. Wang, K.Y. Optimization study of self-propelled sunflower coated seeder cavitator. Master, Inner Mongolia University, 2023.
10. Yuan, X.L. Optimization Design and Experiment of the Suspended Cup Planting Mechanism of Vegetable Transplanter. Master, Southwest University, 2023.
11. Shi, L.R.Z., W. Y.; Sun, W.; Li, R. B.; Xin, B. B.; Dai, F. Development and experiment of electric driving insert hill-drop planter on film for plot corn. *Transactions of the CSAE* **2017**, *33*, 32-38, doi:10.11975/j.issn.1002-6819.2017.04.005.
12. Zhang, X.J.C., Y.; Shi, Z. L.; Jin, W.; Zhang, H. T.; Fu, H.; Wang, D. J. Design and experiment of double-storage turntable cotton vertical disc hole seeding and metering device. *Transactions of the CSAE* **2021**, *37*, 27-36, doi:10.11975/j.issn.1002-6819.2021.19.004.

13. Wang, L.H., X. W.; Hu, C.; Shi, L.; Wang, X. F.; He, Y. C.; Tang, Z. H. Simulation and Experiment for Seeding Performance of Socket Cotton Dibbler Based on Discrete Element Method. *Journal of Agricultural Mechanization Research* **2021**, *43*, 151-156, doi:10.13427/j.cnki.njyi.2021.01.027.
14. Xu, Z.Y.Z., Y.; Hu, M. J.; Ke, H. B.; Zhang, M. Y.; Lü, W. Seeding simulation test of inside-filling cotton seed-metering device based on EDEM. *Journal of GANSU Agricultural University* **2020**, *55*, 175-183, doi:10.13432/j.cnki.jgsau.2020.04.025.
15. Wang, G. Design and test of duck bill seed-metering device for rice film spreading and hole sowing machine. Master Anhui Agricultural University, 2023.
16. Dong, X.Q.S., C.; Zheng, H. N.; Han, R. Q.; Li, Y. L.; Wang, L. P. C.; Song, J. N.; Wang, J. C. Analysis of soil disturbance process by vibrating subsoiling based on DEM-MBD coupling algorithm. *Transactions of the CSAE* **2022**, *38*, 34-43, doi:10.11975/j.issn.1002-6819.2022.01.004.
17. Tan, B.F.D., H. B.; Fu, J.; Sun, H. J.; Cai, X. K.; Li, Z. L. Performance simulation of triangle Chain cup-spoon potato seed feeder based on RecurDyn-EDEM coupling. *Journal of GANSU Agricultural University* **2023**, *58*, 218-227, doi:10.13432/j.cnki.jgsau.2023.03.027.
18. Wang, S.J.Y., Y.; Yu, S. F.; Hou, L. Dynamic analysis on loader coupling based on RecurDyn-EDEM. *Journal of Machine Design* **2021**, *38*, 1-6, doi:10.13841/j.cnki.jxsj.2021.11.002.
19. Cai, Y.Q.L., X. Hu, B.; Mao, Z. B.; Li, J. W.; Guo, M. Y.; Wang, J. Theoretical and experimental analyses of high-speed seed filling in limited gear-shaped side space of cotton precision dibbler *Computers and Electronics in Agriculture* **2022**, *200*, doi:https://doi.org/10.1016/j.compag.2022.107202.
20. Shi, Y.Y.X., R. S.; Wang, X. H.; Hu, Z. H.; David, N.; Ding, W. M. Numerical simulation and field tests of minimum-tillage planter with straw smashing and strip laying based on EDEM software. *Computers and Electronics in Agriculture* **2019**, *166*, doi:https://doi.org/10.1016/j.compag.2019.105021.
21. Wang, Z.Z., W. Y.; Shi, L. R.; Sun, B. G.; Sun, W.; Dai, F.; Zhou, G.; Guo, J. H.; Rao, G.; Li, H. Optimization of the motion parameters of a rolling spoon type precision hole planter based on DEM-MBD coupling. *Journal of China Agricultural University* **2024**, *29*, 66-77, doi:10.11841/j.issn.1007-4333.2024.01.06.
22. Lai, Q.H.J., G. X.; Su, X.; Zhao, L. J.; Qiu, X. B.; Lü, Q. Design and Test of Chain-spoon Type Precision Seed-metering Device for Ginseng Based on DEM-MBD Coupling. *Transactions of the Chinese Society for Agricultural Machinery* **2022**, *53*, 91-104, doi:10.6041/i.issn.1000-1298.2022.03.009.
23. Liu, L. Study on crawl-soil Interaction of deep-sea harvester based on Recurdyn-DEM. Master, Chang'an University, 2023.
24. Yang, W.C.P., W.; Pan, W. J.; Zhang, X. W.; Zhang, L.; Zheng, J. X. Design and experiment of soil covering andcompacting device for Panax notoginseng seedling sowing. *Journal of South China Agricultural University* **2022**, *43*, 122-132, doi:10.7671/j.issn.1001-411X.202106019.
25. Yan, X.D. Particle modelling of soybean seeds and the simulation analysis and experimental study of the seed-throwing and pressing. Doctor, Jilin University, 2021.
26. Liu, R.L., Y. J.; Liu, C. X.; Liu, L. J. Design and Experiment of Shovel Type Wide Seedling Belt Oat Seeding Furrow Opener. *Transactions of the Chinese Society for Agricultural Machinery* **2021**, *52*, 89-96.
27. Xie, S.Y.Z., X. L.; Liu, F. Y.; Liu, J.; Yuan, X. L.; Liu, W.; Wang, P. Kinetic analysis and experiment of seedling taking and throwing device based on mechanical properties of plug seedlings. *Journal of Jilin University (Engineering and Technology Edition)* **2023**, *53*, 3293-3304, doi:10.13229/j.cnki.jdxbgxb.20220139.
28. Seed sowing machine for the mulching film. **2023**, *JB/T 7732-2023*.
29. Testing methods of single seed drills (precision drills). **2005**, *GB/T 6973-2005*.